

## Contiguous 3d and 4f Magnetism: Strongly Correlated 3d Electrons in YbFe<sub>2</sub>Al<sub>10</sub>

P. Khuntia,<sup>1,\*</sup> P. Peratheepan,<sup>2,3</sup> A. M. Strydom,<sup>1,2</sup> Y. Utsumi,<sup>1</sup> K.-T. Ko,<sup>4</sup> K.-D. Tsuei,<sup>5</sup>  
L. H. Tjeng,<sup>1</sup> F. Steglich,<sup>1</sup> and M. Baenitz<sup>1</sup>

<sup>1</sup>Max Planck Institute for Chemical Physics of Solids, 01187 Dresden, Germany

<sup>2</sup>Highly Correlated Matter Research Group, Physics Department, University of Johannesburg,  
P.O. Box 524, Auckland Park 2006, South Africa

<sup>3</sup>Department of Physics, Eastern University, Vantharumoolai, Chenkalady 30350, Sri Lanka

<sup>4</sup>Max Planck POSTECH Center for Complex Phase Materials, 01187 Dresden, Germany and Pohang 790-784, Korea

<sup>5</sup>National Synchrotron Radiation Research Center, 101 Hsin-Ann Road, Hsinchu 30077, Taiwan

(Received 19 February 2014; published 19 November 2014)

We present magnetization, specific heat, and <sup>27</sup>Al NMR investigations on YbFe<sub>2</sub>Al<sub>10</sub> over a wide range in temperature and magnetic field. The magnetic susceptibility at low temperatures is strongly enhanced at weak magnetic fields, accompanied by a  $\ln(T_0/T)$  divergence of the low- $T$  specific heat coefficient in zero field, which indicates a ground state of correlated electrons. From our hard-x-ray photoemission spectroscopy study, the Yb valence at 50 K is evaluated to be 2.38. The system displays valence fluctuating behavior in the low to intermediate temperature range, whereas above 400 K, Yb<sup>3+</sup> carries a full and stable moment, and Fe carries a moment of about  $3.1\mu_B$ . The enhanced value of the Sommerfeld-Wilson ratio and the dynamic scaling of the spin-lattice relaxation rate divided by  $T^{[27}(1/T_1T)]$  with static susceptibility suggests admixed ferromagnetic correlations.  $^{27}(1/T_1T)$  simultaneously tracks the valence fluctuations from the 4f Yb ions in the high temperature range and field dependent antiferromagnetic correlations among partially Kondo screened Fe 3d moments at low temperature; the latter evolve out of an Yb 4f admixed conduction band.

DOI: [10.1103/PhysRevLett.113.216403](https://doi.org/10.1103/PhysRevLett.113.216403)

PACS numbers: 71.27.+a, 71.10.Hf, 74.40.Kb, 76.60.-k

Novel phases ranging from unconventional superconductivity and spin liquid to quantum criticality in correlated electron systems result from competing interactions between magnetic, charge, orbital, and lattice degrees of freedom [1,2]. Competing interactions such as the mostly antiferromagnetic (AFM) Rudermann-Kittel-Kasuya-Yosida (RKKY) exchange and the Kondo effect on a localized spin may lead to a magnetic instability that generates unusual temperature  $T$  and magnetic field  $H$  scaling behavior of bulk and microscopic observables. The competing magnetic interactions frequently produce generalized non-Fermi-liquid (nFL) scaling in the thermal behavior of physical properties. If the RKKY spin exchange succeeds in overcoming the thermal energy of the spin system conducive to a paramagnetic-to-AFM transition, the addition of a competing Kondo spin exchange with the conduction electrons achieves a curbing effect on the phase transition. Moreover, under favorable conditions such as applied pressure or magnetic field the phase transition may become confined to temperatures arbitrarily close to zero, which in turn leads to remarkable thermal scaling in the realm of quantum criticality [3–7]. In exceptional cases quantum criticality presents itself under ambient conditions, such as in U<sub>2</sub>Pt<sub>2</sub>In [8,9] or in the superconductor  $\beta$ -YbAlB<sub>4</sub> [10]. Quantum criticality stemming from ferromagnetic (FM) exchange on the other hand is a rare occurrence, and has been discussed among 5f-electron systems such as UGe<sub>2</sub> [11,12] or UCoGe [13,14],

4f systems like YbNi<sub>4</sub>(P<sub>1-x</sub>As<sub>x</sub>)<sub>2</sub> [15,16], Ce(Ru<sub>1-x</sub>Fe<sub>x</sub>)PO [17,18], and in weak itinerant ferromagnets like ZrZn<sub>2</sub> [19] and NbFe<sub>2</sub> [20]. YFe<sub>2</sub>Al<sub>10</sub>, an isostructural version of YbFe<sub>2</sub>Al<sub>10</sub> with no 4f electrons, is reported to be a plausible candidate for a FM quantum critical magnet [21–24].

The ternary orthorhombic aluminides of  $RT_2Al_{10}$  type ( $R$  denotes a rare earth element,  $T = Fe, Ru, Os$ ) have been the subject of considerable debate in view of a fascinating conundrum of physical properties. Most notable are the extremes of magnetic interactions found in the Ce series ranging from the unprecedentedly high AFM order at 27 K in CeRu<sub>2</sub>Al<sub>10</sub> [25–28] to the Kondo insulating state in CeFe<sub>2</sub>Al<sub>10</sub> [29]. In the present study to further unravel the nature of the 3d electrons in this class of material, we assess the response of Fe-based magnetism in the presence of localized magnetism, namely the rare earth element Yb, and we use a combination of bulk and microscopic probes due to the anticipated complexity of an admixture of different types of magnetic exchange. A comparable situation can be found in CeFe<sub>2</sub>Al<sub>10</sub> in which the confluence of the two types of magnetic species has the surprising effect of producing the nonmagnetic Kondo insulating state [29], which is an extreme case of local-moment hybridization with the conduction electrons. Recently, there has been a resurgence of research activities in intermediate valence systems following the discovery of superconductivity and quantum critical behavior in an intermediate valence (IV) heavy fermion  $\beta$ -YbAlB<sub>4</sub> [10,30–37].

In this Letter, we present comprehensive magnetic susceptibility, specific heat, and  $^{27}\text{Al}$  NMR investigations on polycrystalline  $\text{YbFe}_2\text{Al}_{10}$ . Furthermore, hard-x-ray photoemission spectroscopy (HAXPES) at SPring-8, Japan was carried out as a direct probe of the valence state of Yb. The magnetic susceptibility and specific heat display low temperature divergences, yet without any signature of magnetic ordering down to 0.35 K. In order to understand the low energy spin dynamics governing the underlying magnetism of the title compound, we have carried out NMR investigations with special attention to the spin-lattice relaxation measurements. The low field spin-lattice relaxation rate shows a divergence towards low temperatures, which is consistent with magnetization and specific heat data. The observed deviations from the Fermi liquid (FL) behavior are associated with correlated 3d Fe moments strongly coupled via the conduction band, which is hybridized with the Yb-derived 4f states.

Polycrystalline samples of  $\text{YbFe}_2\text{Al}_{10}$  have been synthesized following a method discussed elsewhere [22,27]. The dc magnetic susceptibility  $\chi(T)$  [=  $M(T)/H$ ] and thermopower data were obtained using a quantum design, physical property measurement system (QD PPMS).

In a recent work, a Kondo-like electrical resistivity accompanied by divergences in magnetic susceptibility  $\chi(T)$  and the Sommerfeld coefficient  $\gamma(T) = C_p(T)/T$  [where  $C_p(T)$  is the electronic specific heat] in zero field were reported [22] on  $\text{YbFe}_2\text{Al}_{10}$ . The magnetism of Yb in this compound was demonstrated [38] to be subject to an unstable valence and to recover its full trivalent state at  $T > 400$  K, which is in agreement with earlier reports [39].

Shown in Fig. 1(a) is the field dependent magnetic susceptibility  $\chi(T)$  of  $\text{YbFe}_2\text{Al}_{10}$ . The values of  $\chi(T)$  are enhanced by one order of magnitude in comparison with the non-4f electron homologue  $\text{YFe}_2\text{Al}_{10}$  [21], which indicates a strong hybridization of the Yb-derived 4f states with the conduction electron states. A modified band structure is therefore expected with subsequent effects on the itinerant 3d magnetism of Fe. Towards elevated temperatures, Yb tends to reach its full trivalent state and this temperature-driven evolution is appropriately reflected in the thermopower  $S(T)$  i.e., by a broad peak centered at  $T^*$  ( $\approx 100$  K) [see Fig. 1(d)], which we use to denote the temperature scale of the valence change of Yb. Such a peak in thermopower is typical for IV Yb compounds, and our HAXPES study on  $\text{YbFe}_2\text{Al}_{10}$  confirmed such an IV state of Yb in this compound, and the valence of Yb is evaluated to be 2.38 (see the Supplemental Material [40]). At the high temperature end, the consequence of this peak is played out by a change in the sign of  $S(T)$  at about 300 K, which likely implies a temperature-driven change in the relative weights and participation of both holes and electrons in the underlying band structure. This could also be due to the asymmetry of the density of states or the scattering rate at the Fermi energy for a single band. However, the negative sign in  $S(T)$  of  $\text{YbFe}_2\text{Al}_{10}$  signals the stable

and local-moment magnetic character of Yb above 300 K, because  $S(T)$  native to the weakly hybridized  $4f^{13+\delta}$  state of Yb is expected to be negative [47].

The small upturn in  $S(T)$  below 10 K is consistent with the incoherent Kondo-like resistivity  $\rho(T)$  [22]. A peak in  $\rho(T)$  at  $T \approx 4.5$  K (see the Supplemental Material [40], Fig. S1) is reminiscent of Kondo-lattice behavior [22]. The Kondo type upturn in  $\rho(T)$  as well as the low- $T$  divergence in  $\chi(T)$  is quenched by applying magnetic fields of a few teslas. The initial susceptibility  $\chi(H \rightarrow 0)$  at 2 K as well as the high-field magnetization  $M(H)$  yield extremely small values of the magnetic moment in  $\text{YbFe}_2\text{Al}_{10}$ . Following a weak curvature in  $M(H)$  in low fields, there is however no saturation achieved in  $M(H)$  at 2 K even up to 7 T, Fig. 1(c), where a quasilinear-in-field magnetization is found.

A detailed analysis of  $\chi(T)$  [see Fig. 1(b)] reveals an IV state of Yb at low and intermediate  $T$ , but Yb recovers its full moment ( $4.54\mu_B$ ) with a high spin state Fe ( $3.1\mu_B$ ) at  $T > 400$  K with predominant AFM correlations. A similar scenario has been discussed in the IV Yb-based skutterudites  $\text{YbFe}_4\text{Sb}_{12}$  [48] and  $\text{YbFe}_4\text{P}_{12}$  [49]. The deconvolution of the Fe 3d contribution and the more localized Yb 4f contribution is a daunting task and beyond the scope of this Letter. Nonetheless, based on the model of Rajan [50], for the Yb 4f part a constant and  $T$ -independent susceptibility could be expected towards low temperatures. The HAXPES measurement performed with  $h\nu = 6.5$  keV at 50 K confirms the IV state of Yb with valence 2.38 (see the Supplemental Material [40]). Therefore, we assume that the magnetism below 50 K is solely driven by the Fe 3d moments in  $\text{YbFe}_2\text{Al}_{10}$  and we speculate that the Curie-Weiss behavior of  $\chi(T)$  in the intermediate temperature range  $80 \leq T \leq 370$  K is associated with Fe 3d moments with an effective moment of

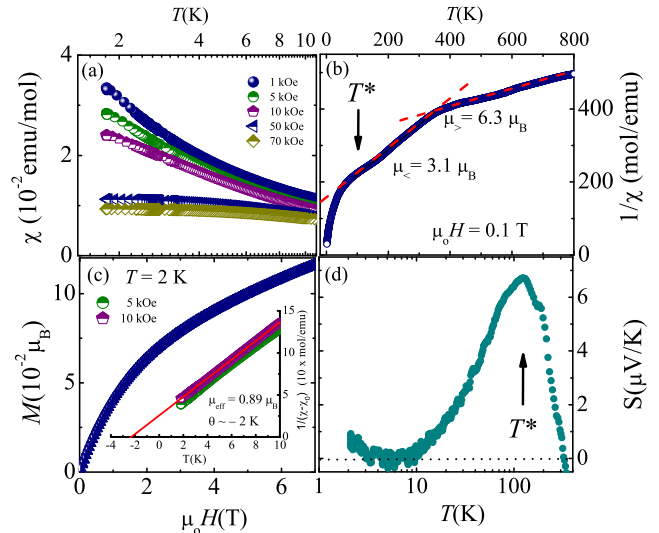


FIG. 1 (color online). (a) Temperature dependence of  $\chi$  in various applied magnetic fields. (b)  $1/\chi$  vs  $T$  at 0.1 T with Curie-Weiss fits. (c) Magnetization isotherm at 2 K; the inset shows  $\chi^{-1}$  vs  $T$  in 5 and 10 kOe with Curie Weiss fit as discussed in the text. (d) Temperature dependence of thermopower.

$3.1/\sqrt{2} = 2.2\mu_B$ . This is in contrast to its non- $4f$  analog  $\text{YFe}_2\text{Al}_{10}$  where Fe carries a much smaller magnetic moment of  $0.35\mu_B$  per Fe [21,23]. This might be related to the difference in charge transfer from the divalent  $\text{Yb}^{2+}$  to the  $\text{Fe}_2\text{Al}_{10}$  host lattice in comparison to the trivalent  $\text{Y}^{3+}$ . The Curie-Weiss behavior of  $\chi(T)$  at  $T \leq 10$  K [see Fig. 1(c), inset] reveals a small Fe moment  $0.89/\sqrt{2} = 0.63\mu_B$  per Fe in  $\text{YbFe}_2\text{Al}_{10}$ . The Weiss temperature of  $\theta \approx -2$  K yields an on-site Kondo temperature of the Fe moments, which amounts to several kelvins [51].

Shown in Fig. 2(a) is the specific heat coefficient  $\gamma(T)$  in different magnetic fields measured using the  $^3\text{He}$  option of QD PPMS. The specific heat coefficient  $\gamma$  is enhanced towards low temperatures and follows a  $\ln(T_0/T)$  behavior with  $T_0 = 2$  K in zero field, which suggests a correlated behavior of electrons. This may be attributed to the entropy of unquenched spin degrees of freedom, or to the impending cooperative behavior at much lower temperatures. Applied magnetic fields achieve a suppression and eventual saturation into a constant value of  $C_p/T$  and thus the recovery of the Fermi liquid ground state. The ratio of the enhanced  $\gamma_0$  value at zero field to the fully quenched value  $\gamma_H$  in 9 T at 0.35 K is about 2.5. Surprisingly, this enhancement factor is qualitatively similar to that of the non- $4f$  compound  $\text{YFe}_2\text{Al}_{10}$  [38]. Despite the fact that the relative enhancements  $\Delta\gamma/\gamma_H = (\gamma_0 - \gamma_H)/\gamma_H$  are similar, it should be mentioned that the  $T$  dependencies of  $C_p/T$  are dissimilar: [ $\ln(T_0/T)$  for  $\text{YbFe}_2\text{Al}_{10}$  and power law behavior in the case of  $\text{YFe}_2\text{Al}_{10}$ ]. For  $\text{YbFe}_2\text{Al}_{10}$  the magnetic entropy ( $0.014R \ln 2$ ) below 2 K is about 3 times larger than its non- $4f$  counterpart  $\text{YFe}_2\text{Al}_{10}$ . Therefore, we relate the low-temperature divergence of the Sommerfeld coefficient to the emergence of correlations among Fe moments amplified by the strong hybridization between Yb  $4f$  states and  $s + d$  conduction band states at the Fermi level. The

field dependence of the Sommerfeld coefficient at 0.5 K follows a  $H^{-0.35}$  behavior [Fig. 2(b)], and the transition to a constant-in- $T$  regime provides the crossover scale between FL and nFL behavior [inset of Fig. 2(b)].

The residual quenched Sommerfeld coefficient of  $\gamma_H = 75.3$  mJ/mol K<sup>2</sup> in  $\text{YbFe}_2\text{Al}_{10}$  exceeds that of the La equivalent [29] by a factor  $\sim 3$ , which indicates that the Fermi level in  $\text{YbFe}_2\text{Al}_{10}$  is occupied predominantly by heavy charge carriers. An enhanced value of the Sommerfeld-Wilson ratio  $R_W = (\pi^2 k_B^2 / \mu_0 \mu_{\text{eff}}) (\chi / \gamma) \approx 12$  at 2 K indicates the presence of FM correlations. It is worth mentioning that there is a striking similarity of  $\text{YbFe}_2\text{Al}_{10}$  specific heat data shown in Fig. 2(a) to those of  $\beta\text{-YbAlB}_4$  [10], which is a rare example of an IV system with local moment low- $T$  electron correlations [36]. Another prominent example in that context is the IV metal  $\text{YbAl}_3$  [52].

$^{27}\text{Al}$ -NMR ( $I = 5/2$ ) measurements have been performed using a standard Tecmag NMR spectrometer in the temperature range  $1.8 \leq T \leq 300$  K and in the field range  $0.98 \leq \mu_0 H \leq 7.27$  T. The orthorhombic crystal structure of  $\text{YbFe}_2\text{Al}_{10}$  hosts five inequivalent Al sites. Usually this results in rather broad NMR spectra with a clear central transition and superimposed first order satellite transitions (see Fig. 3). Surprisingly, we found a rather well-resolved central transition with a small field dependent anisotropy, which implies that the different Al sites are rather equal in their magnetic environment [21,38].

The sharp central transition enables us to perform  $^{27}\text{Al}$  spin-lattice relaxation rate (SLRR) measurements consistently following a saturation recovery method with suitable rf pulses, and the results are shown in Fig. 4. The relaxation rate divided by  $T$ , i.e.,  $1/T_1 T$ , shows a divergence towards low temperatures [Fig. 4(a)] with a proportionality  $\chi(T)/\sqrt{T}$  in the lowest magnetic fields. Such a dynamic scaling is frequently found in heavy fermion systems with

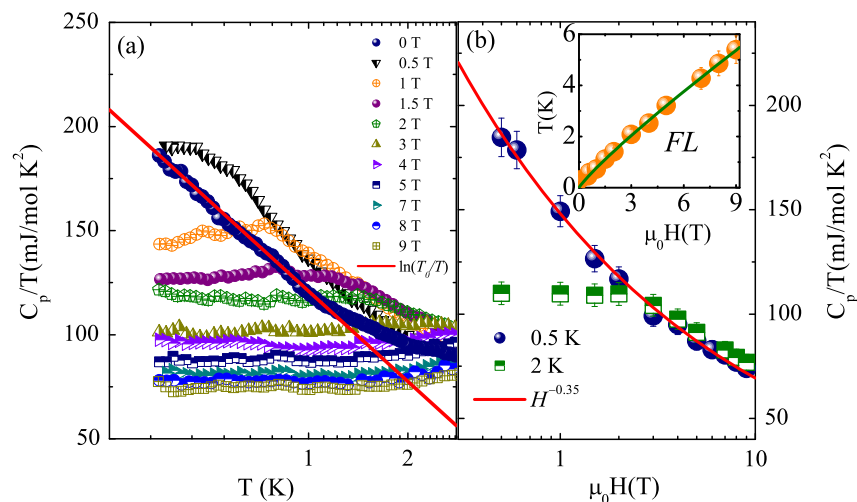


FIG. 2 (color online). (a) Temperature dependence of specific heat coefficients taken in different applied magnetic fields. The solid line is a fit to  $\ln(T_0/T)$  with  $T_0 = 2$  K. (b)  $C_p(T)/T$  vs  $\mu_0 H$  at 0.5 and 2 K, with solid line a fit to  $H^{-0.35}$ . The inset shows the field dependence of the crossover temperature (to FL behavior) obtained from  $C_p(T)/T$ .

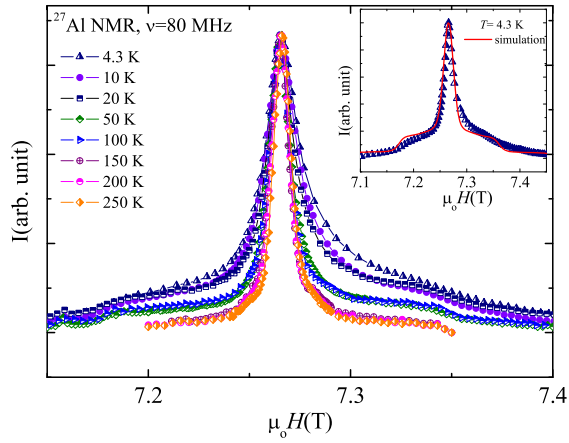


FIG. 3 (color online).  $^{27}\text{Al}$  NMR spectra at 80 MHz for different temperatures. The inset shows the simulation of the 4.3 K spectra.

AFM correlations and even with admixed FM correlations as in CeFePO [53–55]. In addition, the relative change  $[(\gamma_0 - \gamma_H)/\gamma_H]^2 = 1.7$  underestimates the SLRR enhancement found in the experiment ( $\approx 4.6$ ). The stronger enhancement in the SLRR points towards the presence of dominant  $q = 0$  contributions, as a response to FM correlations. Usually the specific heat is more sensitive to finite  $q$  excitations, which explains the difference in the enhancement factors. In contrast with the discrepancy in the  $T$  enhancement, the field dependence of the SLRR is in agreement with the Fermi liquid theory exhibiting  $1/T_1 T \sim (C/T)^2 \sim \gamma^2$  behavior. Here a power law  $H^{-0.35}$  is found for the Sommerfeld coefficient which implies a power law  $H^{-0.7}$  for the SLRR. This field dependence is indeed found for the SLRR at 2.5 K [see Fig. 4(b) with  $H^{-0.77}$ ], which is further supported by  $1/T_1 T \sim \chi^2$  behavior commonly found in local-moment metals and is in contrast to that observed in  $\text{YFe}_2\text{Al}_{10}$  [21].

Independent of the magnetic field a peak [Fig. 4(a)] in the SLRR at  $T^*$  ( $\approx 100$  K) signals the onset of valence

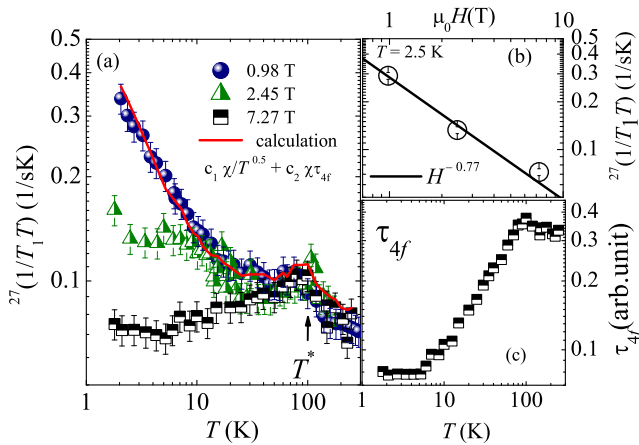


FIG. 4 (color online). (a)  $^{27}(1/T_1 T)$  vs  $T$  in different applied magnetic fields. The solid line is the calculated value as discussed in the text. (b) The field dependence of  $^{27}(1/T_1 T)$  at 2.5 K with a fit to  $H^{-0.77}$ . (c) The temperature dependence of  $\tau_{4f}$  at 7.27 T.

fluctuations in the SLRR of the Al nuclei at high  $T$ . In general the SLRR probes the  $q$ -averaged low lying excitations in the spin fluctuation spectra and  $1/T_1 T$  can be expressed as;  $\frac{1}{T_1 T} \propto \sum_q |A_{\text{hf}}(q)|^2 (\chi''(q, \omega_n)/\omega_n)$ , where  $A_{\text{hf}}(q)$  is the  $q$ -dependent form factor of the hyperfine interactions and  $\chi''(q, \omega_n)$  is the imaginary part of the dynamic electron spin susceptibility [56,57]. In the presence of  $q$ -isotropic  $4f$  fluctuations of IV Yb coexisting with  $q = 0$  FM  $3d$  correlations, the SLRR could be approximated by  $(1/T_1 T) \approx A_{\text{hf}}^2 \chi_0 [\tau_{3d} + \tau_{4f}]$ , where  $\tau_{4f} (= 1/\Gamma_{4f})$  is the effective fluctuation time of the  $4f$  ion,  $\tau_{3d} (= 1/\Gamma_{3d})$  is the effective fluctuation time of the  $3d$  ion ( $\Gamma_{4f,3d}$  are corresponding dynamic relaxation rates), and  $\chi_0$  is the uniform bulk susceptibility. It has to be mentioned that in case of large valence variations (as in Eu systems where the valence could vary between 2+ and 3+) the electronic structure may be perturbed, which changes  $A_{\text{hf}}$ , but we omit this detail for  $\text{YbFe}_2\text{Al}_{10}$  and assume that  $A_{\text{hf}}$  is not varying with temperature.

The beauty of these results is that  $^{27}\text{Al}$  NMR simultaneously senses the valence fluctuations from the  $4f$  Yb ions in the high  $T$  range and the low  $T$  field dependent Kondo-like correlations associated with the  $3d$  Fe ions. Upon the application of high magnetic fields these fluctuations are quenched (here  $\tau_{3d} \ll \tau_{4f}$  for all  $T$ ). Therefore, the relaxation rate at 7.27 T allows for the determination of the effective fluctuation time  $\tau_{4f} = 1/\Gamma_{4f}$ , which is plotted as a function of temperature in Fig. 4(c). The steplike change of  $\tau_{4f}$  at about 100 K signals more a charge gap scenario (as in Kondo insulators) than an intermediate valence system with a smooth variation in  $\tau_{4f}$ . With the knowledge of the  $T$ -dependent (but not  $H$ -dependent) relaxation time  $\tau_{4f}$ , we now proceed to fit the  $1/T_1 T$  vs  $T$  results in a low magnetic field. Surprisingly, the assumption of  $\tau_{3d} = 1/\sqrt{T} \propto \chi$  results in a very good agreement with the experimental data [red line in Fig. 4(a)], which also explains the  $^{27}(1/T_1 T) \propto \chi^2$  behavior at the  $T \rightarrow 0$  limit. With this approach we have convincingly shown that NMR is able to probe both energy regimes: (i) the high-temperature IV regime where  $\Gamma_{4f}$  is changing strongly, and (ii) the low- $T$  regime where  $\Gamma_{4f}$  is constant and  $\Gamma_{3d}$  shows a local moment behavior with  $\Gamma_{3d} \propto \sqrt{T}$ .

In conclusion, we have found an unexpected localization of Fe-derived  $3d$  states upon cooling  $\text{YbFe}_2\text{Al}_{10}$  to helium temperatures. As in this material the Yb-derived  $4f$  electrons form a nonmagnetic, intermediate-valent state at low temperatures (with a Yb valence of 2.38), the observed Kondo-lattice behavior has to be attributed to the localized  $3d$  electrons. Because of the low on-site Kondo scale of  $T_0 \approx 2$  K, one would expect the  $3d$  magnetic moments to be subject to some kind of long-range ordering [58]. However, this appears to be avoided, at least above 0.4 K, by a competition between ferro- and antiferromagnetic correlations, which have been inferred from a strongly enhanced Sommerfeld-Wilson ratio on the one hand and the field dependencies of the specific heat and spin-lattice relaxation rate on the other.

We thank C. Geibel, A. P. Mackenzie, H. Yasuoka, M. C. Aronson, M. Brando, and M. Garst for fruitful discussions. We thank C. Klausnitzer for technical support concerning the specific heat measurements. We thank the Deutsche Forschungsgemeinschaft for financial support (Project No. OE-511/1-1). A. M. S. acknowledges support from South Africa's National Research Foundation (78832).

\*pkhuntia@gmail.com

- [1] S. Sachdev, *Quantum Phase Transitions* (Cambridge University Press, Cambridge, England, 1999).
- [2] P. Gegenwart, Q. Si, and F. Steglich, *Nat. Phys.* **4**, 186 (2008).
- [3] G. R. Stewart, *Rev. Mod. Phys.* **73**, 797 (2001).
- [4] G. R. Stewart, *Rev. Mod. Phys.* **78**, 743 (2006).
- [5] H. v. Löhneysen and P. Wölfle, *Rev. Mod. Phys.* **79**, 1015 (2007).
- [6] M. Brian Maple, R. E. Baumbach, N. P. Butch, J. J. Hamlin, and M. Janoschek, *J. Low Temp. Phys.* **161**, 4 (2010).
- [7] Q. Si and F. Steglich, *Science* **329**, 1161 (2010).
- [8] A. Strydom and P. de V. Du Plessis, *Physica (Amsterdam)* **223–224B**, 222 (1996).
- [9] P. Estrela, A. de Visser, F. R. de Boer, G. J. Nieuwenhuys, L. C. J. Pereira, and M. Almeida, *Physica (Amsterdam)* **259–261B**, 409 (1999).
- [10] S. Nakatsuji *et al.*, *Nat. Phys.* **4**, 603 (2008).
- [11] S. Saxena *et al.*, *Nature (London)* **406**, 587 (2000).
- [12] H. Kotegawa, V. Taufour, D. Aoki, G. Knebel, and J. Flouquet, *J. Phys. Soc. Jpn.* **80**, 083703 (2011).
- [13] E. Slooten, T. Naka, A. Gasparini, Y. K. Huang, and A. de Visser, *Phys. Rev. Lett.* **103**, 097003 (2009).
- [14] T. Hattori *et al.*, *Phys. Rev. Lett.* **108**, 066403 (2012).
- [15] R. Sarkar, P. Khuntia, C. Krellner, C. Geibel, F. Steglich, and M. Baenitz, *Phys. Rev. B* **85**, 140409(R) (2012).
- [16] A. Steppke *et al.*, *Science* **339**, 933 (2013).
- [17] S. Kitagawa, K. Ishida, T. Nakamura, M. Matoba, and Y. Kamihara, *Phys. Rev. Lett.* **109**, 227004 (2012).
- [18] S. Kitagawa, K. Ishida, T. Nakamura, M. Matoba, and Y. Kamihara, *J. Phys. Soc. Jpn.* **82**, 033704 (2013).
- [19] R. P. Smith, M. Sutherland, G. G. Lonzarich, S. S. Saxena, N. Kimura, S. Takashima, M. Nohara, and H. Takagi, *Nature (London)* **455**, 1220 (2008).
- [20] M. Brando, W. Duncan, D. Moroni-Klementowicz, C. Albrecht, D. Grüner, R. Ballou, and F. Grosche, *Phys. Rev. Lett.* **101**, 026401 (2008).
- [21] P. Khuntia, A. M. Strydom, L. S. Wu, M. C. Aronson, F. Steglich, and M. Baenitz, *Phys. Rev. B* **86**, 220401(R) (2012).
- [22] A. M. Strydom and P. Peratheepan, *Phys. Status Solidi RRL* **4**, 356 (2010).
- [23] K. Park, L. S. Wu, Y. Janssen, M. S. Kim, C. Marques, and M. C. Aronson, *Phys. Rev. B* **84**, 094425 (2011).
- [24] A. M. Strydom, P. Khuntia, M. Baenitz, P. Peratheepan, and F. Steglich, *Phys. Status Solidi B* **250**, 630 (2013).
- [25] C. S. Lue, S. H. Yang, A. C. Abhyankar, Y. D. Hsu, H. T. Hong, and Y. K. Kuo, *Phys. Rev. B* **82**, 045111 (2010).
- [26] S. C. Chen and C. S. Lue, *Phys. Rev. B* **81**, 075113 (2010).
- [27] A. M. Strydom, *Physica (Amsterdam)* **404B**, 2981 (2009).
- [28] D. D. Khalyavin *et al.*, *Phys. Rev. B* **82**, 100405(R) (2010).
- [29] Y. Muro, K. Motoya, Y. Saiga, and T. Takabatake, *J. Phys. Soc. Jpn.* **78**, 083707 (2009).
- [30] S. Watanabe and K. Miyake, *J. Phys. Condens. Matter* **24**, 294208 (2012).
- [31] D. T. Adroja and S. K. Malik, *J. Magn. Magn. Mater.* **100**, 126 (1991).
- [32] S. Patil, R. Nagarajan, C. Godart, J. Kappler, L. Gupta, B. Padalia, and R. Vijayaraghavan, *Phys. Rev. B* **47**, 8794 (1993).
- [33] Y. Matsumoto, S. Nakatsuji, K. Kuga, Y. Karaki, N. Horie, Y. Shimura, T. Sakakibara, A. H. Nevidomskyy, and P. Coleman, *Science* **331**, 316 (2011).
- [34] M. Okawa *et al.*, *Phys. Rev. Lett.* **104**, 247201(2010).
- [35] A. H. Nevidomskyy and P. Coleman, *Phys. Rev. Lett.* **102**, 077202 (2009).
- [36] L. M. Holanda, J. M. Vargas, W. Iwamoto, C. Rettori, S. Nakatsuji, K. Kuga, Z. Fisk, S. B. Oseroff, and P. G. Pagliuso, *Phys. Rev. Lett.* **107**, 026402 (2011).
- [37] W. Schnelle, A. Leithe-Jasper, H. Rosner, R. Cardoso-Gil, R. Gumenuik, D. Trots, J. Mydosh, and Yu. Grin, *Phys. Rev. B* **77**, 094421 (2008).
- [38] P. Khuntia, A. Strydom, F. Steglich, and M. Baenitz, *Phys. Status Solidi B* **250**, 525 (2013).
- [39] V. M. T. Thiede, T. Ebel, and W. Jeitschko, *J. Mater. Chem.* **8**, 125 (1998).
- [40] See Supplemental Material at <http://link.aps.org/supplemental/10.1103/PhysRevLett.113.216403>, which includes Refs. [21,24,34,38,39,41–46], for experimental details and results on magnetization, resistivity, specific heat, NMR, and HAXPES.
- [41] D. R. Hamann, *Phys. Rev.* **158**, 570 (1967).
- [42] T. A. Costi, *Phys. Rev. Lett.* **85**, 1504 (2000).
- [43] T. A. Costi, A. C. Hewson, and V. Zlatić, *J. Phys. Condens. Matter* **6**, 2519 (1994).
- [44] W. Felsch and K. Winzer, *Solid State Commun.* **13**, 569 (1973).
- [45] E. S. R. Gopal, *Specific Heat at Low Temperatures* (Plenum Press, New York, 1966).
- [46] A. Narath, *Phys. Rev.* **162**, 320 (1967).
- [47] K. Behnia, D. Jaccard, and J. Flouquet, *J. Phys. Condens. Matter* **16**, 5187 (2004).
- [48] W. Schnelle, A. Leithe-Jasper, M. Schmidt, H. Rosner, H. Borrmann, U. Burkhardt, J. Mydosh, and Y. Grin, *Phys. Rev. B* **72**, 020402(R) (2005).
- [49] A. Yamamoto, S. Wada, I. Shirotnani, and C. Sekine, *J. Phys. Soc. Jpn.* **75**, 063703 (2006).
- [50] V. T. Rajan, *Phys. Rev. Lett.* **51**, 308 (1983).
- [51] A. J. Heeger, in *Solid State Physics: Advances in Research and Applications*, edited by F. Seitz, D. Turnbull, and H. Ehrenreich (Academic, New York, 1969), Vol. 23, p. 283.
- [52] U. Walter, E. Holland-Moritz, and Z. Fisk, *Phys. Rev. B* **43**, 320 (1991).
- [53] D. L. Cox, N. E. Bickers, and J. W. Wilkins, *J. Appl. Phys.* **57**, 3166 (1985).
- [54] N. Büttgen, R. Böhmer, A. Krimmel, and A. Loidl, *Phys. Rev. B* **53**, 5557 (1996).
- [55] E. M. Brüning, C. Krellner, M. Baenitz, A. Jesche, F. Steglich, and C. Geibel, *Phys. Rev. Lett.* **101**, 117206 (2008).
- [56] T. Moriya, *Spin Fluctuations in Itinerant Electron Magnetism* (Springer-Verlag, Berlin, 1985).
- [57] Y. Kuramoto and Y. Kitaoka, *Dynamics of Heavy Electrons* (Oxford, New York, 2000).
- [58] V. Yu. Irkhin and M. I. Katsnelson, *Phys. Rev. B* **56**, 8109 (1997).